SANDING OF *FAGUS SILVATICA L.* WOOD PERPENDICULARLY TO THE GRAINS

Bolesław Porankiewicz[a*] and Grzegorz Wieloch[b]

In this paper the dependencies of the degree of surface burning and intensity during disc sanding perpendicular to the wood grains of *Fagus silvatica L.* were examined for several machining parameters. Significant impacts of sanding load, thickness, and width of a wooden specimen on the surface burning and disc sanding intensity were evidenced and analyzed by evaluation of multi-factor, non-linear relations. Less important influences of cutting speed and size of grit on the surface burning and the sanding intensity, as well as single sanding cycle time and total sanding operating time on the surface burning were observed.

Keywords: Disc sanding; Fagus silvatica L; Sanding intensity; Surface burn; Statistical dependencies

*Contact information: a: Dr. Hab. Emeritus; b: Agricultural University of Poznań, Wojska Polskiego 28, 60 637 Poznań, Poland; *Corresponding author: poranek@amu.edu.pl*

INTRODUCTION

When a sanding process is carried out perpendicularly to the grains of the wood of *Fagus silvatica L.*, especially in the case of small-dimension work pieces, certain troubles may be caused due to sufficiently intense generation of heat. Unacceptable surface burning marks may result as a consequence of any attempt to speed up the process by increasing the sanding load Q_S. Many studies from the field of wood sanding, mostly related to band sanding, concentrate on a direction parallel or transverse to wood grains, where the problem mentioned above, under the same (acceptable) sanding pressure p_S, was not considered (Pahlitzsch and Dziobek 1961; Orlicz 1982). However, the possibility of burning of a tool in a context of overly intensive contact during wide-band wood sanding has been mentioned in the literature (Schmutzler 1961).

The present study was prompted by observations of burning marks during production of secondary wood items at a no-longer existing factory. The goal is to evaluate dependencies of the state of surface of wood specimen after sanding, as defined by degree of burning *dB* and the disc sanding intensity $\Delta l_{WP}/\Delta t_S$, upon several machining parameters. A further objective was to determine what sanding parameters have to be applied to avoid burning marks on the surface of wooden specimen and achieve the most effective sanding process perpendicularly to grains of *Fagus silvatica L.*

EXPERIMENTAL

Experiments were done on a DCXA disc sanding machine at the Agricultural University of Poznań woodworking machinery laboratory, under following sanding

conditions (where the values in brackets "< >" show the minimum and maximum values of independent variables, and " .." marks show that many variables in a range were analyzed):

1. Nominal power of electrical motor N_S = 4 kW.
2. Sanding disc rotational speed n = 970 min^{-1}.
3. Radius of disc sanding tool r_S < 34 .. 242 > mm.
4. Sanding speed v_C < 3.5 .. 24.6 > m/s.
5. Time of single sanding cycle t_S < 0.067 .. 3 > min.
6. Total operating time of a sanding tool Σt_S < 3 .. 330 > min.
7. Sanding load Q_S < 1.2 .. 196.9 > N.
8. Sanding pressure p_S < 0.0015 .. 0.0335 > MPa.
9. Number of grit of the electrocorunde sanding tool *no.* < 12(100); 50(30); 160(12) >.
10. Size of single grit of the electrocorunde sanding tool R_{SP} < 0.14; 0.57; 1.67 > mm.
11. Round-up of a top of single grit of the electrocorunde sanding tool ρ_{SP} < 0.02; 0.083; 0.23 > mm.
12. Static, axial run-out a_R of working surface of sanding disc, described by formula (1).

$$a_R = 0.0023\ r_S \quad (1)$$

13. Thickness of the wooden specimen g_{WP} < 11.7 .. 71.3 > mm.
14. Width of the wooden specimen b_{WP} < 35.6 .. 144.1 > mm.
15. Area of the wooden specimen sanded A_S < 785 .. 5881 > mm^2.

Physical properties of wood of *Fagus silvatica L*, originating from Great Poland province, Poland, Europe.

16. Moisture content of the wooden specimen mc_{WP} < 5; 8 > %.
17. Density of the wooden specimen D_{WP} = 790 kg/m^3.

The choice of the type of machine, the wood species, and the sanding direction was done according to direct inquiry of personnel at a secondary wood products factory. Sanding experiments were performed on the test stand shown in Fig. 1. The disc sanding machine DCXA was equipped with an individual dust exhauster. The wooden specimen was freely pressed to the sanding tool between aluminum slide guides mounted to the machine table on the left and right sides, at the chosen positions, giving an average sanding radius r_S. The sanding load Q_S was realized with use of weights and bowl, hanging on a 0.5 or 1 mm thick bend, directed by two pairs of rolls, fixed to aluminum slides, mounted on the left and right sides of the wooden specimen. A bend having a 0.5 mm thickness was used for loads up to 29 N. A width of the wooden specimen b_{WP} defined the minimum and maximum sanding speed v_C. The static, axial run-out a_R of the sanding tool mounted to the sanding disc are collected in Table 1.

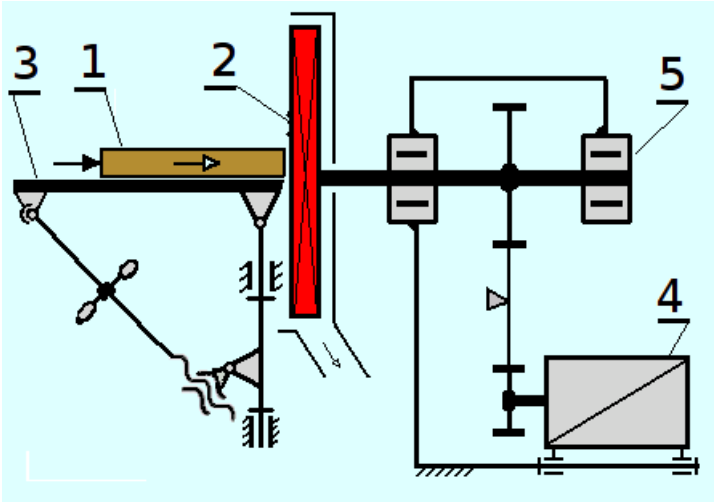

Fig. 1. Scheme of the test stand on disc sanding machine: 1 – Wooden specimen; 2 – Sanding tool; 3 – Machine table, adjustable; 4 – Electrical motor; 5 – Bearing

Table 1. Axial, Static Run-Out a_R (mm) of a Sanding Tool, for Different Sanding Grit *no.*, Sanding Radius r_S and Sanding Load Q_S

r_S	Grit *no. 160*(12)				Grit *no.* 50(30)				Grit *no.* 12(100)			
(mm)	For Q_S (N)											
	3.19	5.15	8.09	13	3.19	5.15	8.09	13	3.19	5.15	8.09	13
66	0.13	0.18	0.18	0.18								
135	0.41	0.4	0.4	0.4								
200	0.96	0.80	0.5	0.5								
242	1.1	0.75	0.7	0.6	0.29	0.34	0.42	0.42	0.36	0.38	0.38	0.4

The numbering of the sanding grit is not precise. It differs slightly between standards ANSI (American National Standard Institute) B74.18-1984, DIN (Deutsches Institute fur Normung) 69176, FEPA (Federation Europenne des Fabricants de Produits Abrasifs) Standard 43-D-1984, JIS (Japanese Industrial Standard) R 6001-1973, and PN (Polska Norma) -76/M-59107. For this reason it was decided to evaluate a maximum R_{SPX} and average size R_{SP} of the grit, as well as the round-up ρ_{SP} of a top of a grit for analyzed sanding tools, for a 50 mm section of a bended up sanding tool, projected on a shield of tool microscope BMI, under magnification 30^X. Results of these measurements, collected in Table 2, show that small sanding grit analyzed in the experiment was sharper in comparison to larger grit. The relationship between the ρ_{SP} and the average size R_{SP} of grit can be described by formula (2).

$$\rho_{SP} = 0.1436\, R_{SP}^{0.9344} \quad \text{(mm)} \qquad (2)$$

Table 2. Parameters of Sanding Tools (sanding papers)

Grit *no.*	R_{SPX}	R_{SP} (mm)	ρ_{SP}
160(12)	1.97	1.67	0.230
50(30)	0.70	0.57	0.083
12(100)	0.19	0.14	0.027

For metering of the sanding time t_S, a chronometer with accuracy of 1s was used. After every sanding cycle, the sanded specimens' state surface was visually checked from the point of view of the degree of burning, according to scale shown in Table 3. The degree of burning represents a range, <1, 6>. Differentiation of color zones of sanded surface after every test, as shown in Table 3, can be seen.

Table 3. The Scale of the Degree Burning *dB* of Sanded Surface

No burning marks Natural colour of wood on whole sanded surface	Minor burning marks Narrow, light - brown zones between natural colour of a wood	Light burning marks Wide, light - brown zones between natural colour of a wood	Medium burning marks Narrow, dark - brown zones between natural colour of a wood	Strong burning marks Black zones between dark brown background	Very strong burning marks Black colour on whole sanded surface
1	2	3	4	5	6
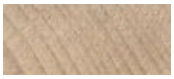	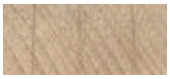		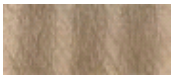	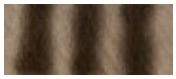	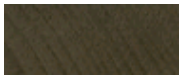

Loss of the wooden specimen length Δl_{WP} after a sanding cycle was estimated for three points, with use of an outer screw micrometer, with an accuracy of 0.01 mm, after 10 min of cooling down. Large weight changes of the wooden specimen, associated with significant heat generation and moisture movement in the sanding zone, rendered the use of a balance inappropriate.

A statistical model, of relation $dB = f(p_S, g_{WP}, v_C, \rho_{SP}, R_{SP}, t_S, \Sigma t_S, a_R)$ and $\Delta l_{WP}/\Delta t_S = f(Q_S, g_{WP}, b_{WP}, v_C, \rho_{SP}, R_{SP}, \Sigma t_S, a_R)$ should fit an experimental matrix by the lowest summation of residuals square S_K, by the lowest standard deviation S_D, and by the highest correlation coefficient R between predicted and observed values. It is also very important to get the proper influence of variables analyzed, especially in case of an incomplete experimental matrix. Usually the use of simpler models results in decreasing approximation quality (larger S_K and S_D, and lower R) and also a reverse impact of low-importance variables. One has to remember that such a statistical relationship is valid only for ranges of independent variables defined in the experimental matrix. Significant error may be associated with points outside of the analyzed range of independent variables, especially in the evaluation of models with interactions, as well as in cases of incomplete experimental matrices. In case of several studies done under the same machining conditions, a discussion of a choice of mathematical model seems to be valuable. In the evaluation process of statistical dependencies $dB = f(p_S, g_{WP}, v_C, \rho_{SP}, R_{SP}, t_S, \Sigma t_S, a_R)$ and

$\Delta l_{WP}/\Delta t_S = f(Q_S, g_{WP}, b_{WP}, v_C, \rho_{SP}, R_{SP}, \Sigma t_S, a_R)$, linear functions, second order multinomial formulas, as well as power-type and exponential functions without and with interactions, were analyzed in preliminary calculations. According to the assumptions discussed earlier, the most adequate models appeared to be those represented by the equations (3) and (4). In the formula (4), the thickness g_{WP} and the width b_{WP} of the work piece have to be expressed in cm.

$$dB = c_1 t_S^{c_2} \bullet \rho_{SP}^{c_3} \bullet R_{SP}^{c_4} \bullet g_{WP}^{c_5} \bullet v_C^{c_6} \bullet p_S^{c_7} \bullet \sum_{k=1}^{k=n} \left[c_8 \bullet e^{c_9 \bullet t_S + c_{10} \bullet p_S + c_{11}} \right] + c_{12} \bullet a_R + c_{13}$$

$$0.5 < dB < 6.5 \qquad (3)$$

where: e is the base of natural logarithms, e = 2,71828182 ...

$$\frac{\Delta l_{WP}}{\Delta t_S} = c_1 \bullet \rho_{SP}^{c_2} \bullet R_{SP}^{c_3} \bullet g_{WP}^{c_4} \bullet b_{WP}^{c_5} \bullet v_C^{c_6} \bullet Q_S^{c_7} + c_8 \bullet \sum t_S + c_9 \bullet a_R + c_{10}$$

$$0 < \Delta l_{WP}/\Delta t_S < 14.68 \text{ (mm/min)} \qquad (4)$$

The model (3) was also unsuccessfully analyzed in relation to the sanding intensity $\Delta l_{WP}/\Delta t_S$ case, considering the combined interaction of sanding parameters analyzed with the total sanding operating time Σt_S. Estimators for equations (3) and (4) were evaluated from an experimental matrix containing 105 measuring points (Table 7), with three repetitions of every test. Several additional tests were done with one repetition. The necessary number of iterations reached 10^{10}. During the evaluation process of models (3) and (4), elimination of unimportant or less important estimators was done by use of a coefficient of relative importance C_{RI}, defined by formula (5), under the assumption that $C_{RI} > 0.1$.

$$C_{RI} = \frac{S_K - S_{KOK}}{S_K} \bullet 100 \ \ (\%) \qquad (5)$$

In formula (5) the new terms are:

S_{K0K} - Summation of square of residuals, by $c_K = 0$.
c_K - K estimator number in statistical model evaluated.

The summation of residuals square S_K, standard deviation S_D, and the square of correlation coefficient of the predicted, and observed values R^2 was used for characterization of approximation quality. Calculations were performed at Poznań Networking & Supercomputing Center PCSS on an SGI Altix 3700 computer, using a special optimization program, based on a least squares method combined with gradient and Monte Carlo methods (Porankiewicz 1988) with further changes.

RESULTS AND DISCUSSION

The following estimators for formula (3) describing the dependence $dB = f(p_S, g_{WP}, v_C, \rho_{SP}, R_{SP}, t_S, \Sigma t_S, a_R)$ were evaluated: $c_1 = 15.6689$; $c_2 = 0.09871$; $c_3 = 0.03613$; $c_4 = 0.11905$; $c_5 = 0.49341$; $c_6 = -0.09756$; $c_7 = 0.26158$; $c_8 = 0.01953$; $c_9 = -901.077$; $c_{10} = -1.8949$; $c_{11} = -0.31743$; $c_{12} = 0.01592$; $c_{13} = -0.80184$. The approximation quality of the formula (3) fit can be characterized by the quantifiers: $S_K = 26.5$; $R = 0.95$; $R^2 = 0.9$; $S_D = 0.5$ and also was illustrated in Figure 2. The coefficients of relatively importance C_{RI} for estimators of formula (3) were as follows: $C_{RI1} = 7125$, $C_{RI2} = 338$, $C_{RI3} = 5$, $C_{RI4} = 792$, $C_{RI5} = 1.1 \cdot 10^6$, $C_{RI6} = 175$, $C_{RI7} = 2035$, $C_{RI8} = 27$, $C_{RI9} = 29096$, $C_{RI10} = 126$, $C_{RI11} = 13$, $C_{RI12} = 7$, $C_{RI13} = 13$.

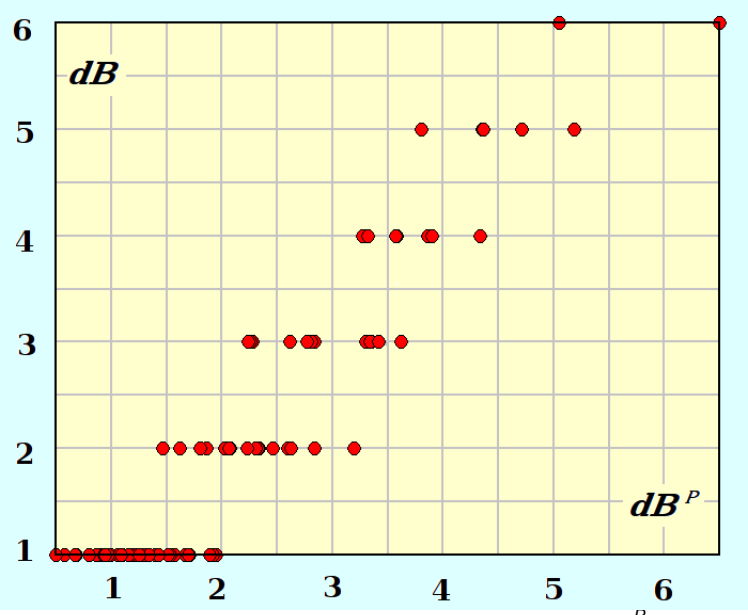

Fig. 2. Plot of the degree of burning *dB* observed, against predicted dB^P, according to formula (3)

An explanation for why the surface of *Fagus silvatica L.* wood became burnt during sanding perpendicularly to grains is that the contact temperature in the sanding zone exceeded a temperature of thermal decomposition of all the wood components, generated by too large a density of the heat input stream q, as high as $q > 0.11$ cal·(s·m·K)$^{-1}$, for a test with observed $dB = 6$. A negative rake angle of all sanding edges and the largest cutting resistance, due to cutting perpendicular to wood grain, as well as very low by coefficient of thermal conductivity, as high as 0.269 cal·(s·m·K)$^{-1}$, support this phenomenon.

Figure 3 shows that the degree of burning *dB* of a sanded surface, for assumed conditions, strongly depended upon the sanding pressure p_S over the whole analyzed range. The colours on the plot indicate the degree of burning *dB* for each of the coordinates. A significant influence of the sanding speed v_C on the degree of burning *dB* could be observed only for large sanding pressure p_S, while for the lowest p_S, this influence was very small.

From Figure 4, it can be seen that increasing the time of a single sanding cycle t_S increased a level of the burning *dB* of the sanded surface. This was due to a larger temperature rise in the contact zone between a wood specimen and a sanding grit.

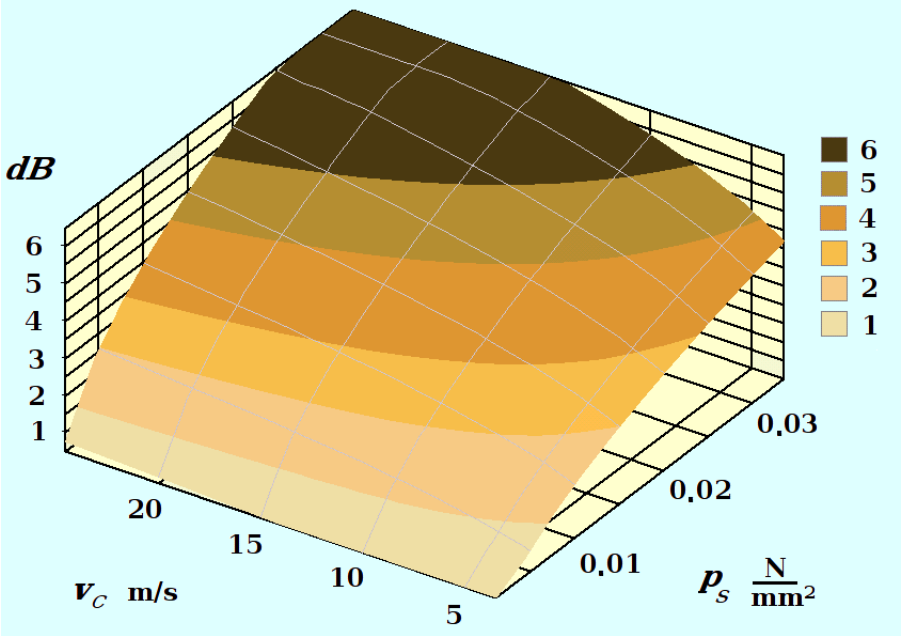

Fig. 3. Dependence between the degree of burning *dB* upon the sanding pressure p_S and the sanding speed v_C, according to formula (3); sanding parameters: g_{WP} = 66.4 mm; b_{WP} = 82.4 mm; t_S = 0.083 min; Σt_S = 0.083 min; a_R = 0.5 mm; R_{SP} = 1.67 mm

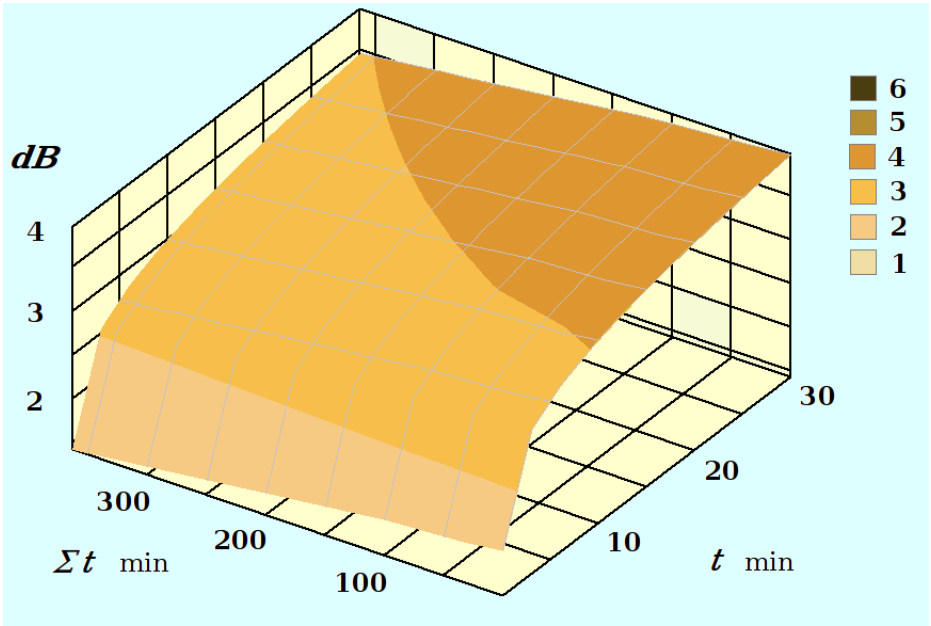

Fig. 4. Dependence between degree of the burning level *dB* upon the time of single sanding cycle t_S and the total sanding operating time Σt_S, according to formula (3); sanding parameters: p_S = 0.004 N/mm^2, g_{WP} = 35 mm, b_{WP} = 82.4 mm, v_C = 24.6 m/s; a_R = 0.5 mm; R_{SP} = 1.67 mm

An increase of the total sanding operating time Σt_S slightly decreased the degree of the burning *dB*. This was due to decreasing sanding capability with increasing amount of debris collected close to the cutting edges on the working surfaces of sanding grits and inside void areas between grits. An increase of the size of sanding grit R_{SP} slightly increased the level of burning *dB* of the sanded surface. This was attributed to the fact that the smaller grit had more sharp edges and generated less heat during sanding. This relationship is expressed in formula (3), combining the influence of the size of sanding grit R_{SP} together with the round-up of the top surfaces of sanding grit ρ_{SP}, defined by statistical formula (2). For this reason the influence of the ρ_{SP} on the level of burning *dB* was not analyzed separately.

An increase of the thickness of the sanding specimen g_{WP} slightly increased the level of burning *dB* of the sanded surface. This was attributed to a longer contact time of a sanding grit with wood. According to formula (3) an increase of the axial run-out b_W of the sanding tool slightly (on a low level of importance) decreased the level of burning *dB* of the sanded surface.

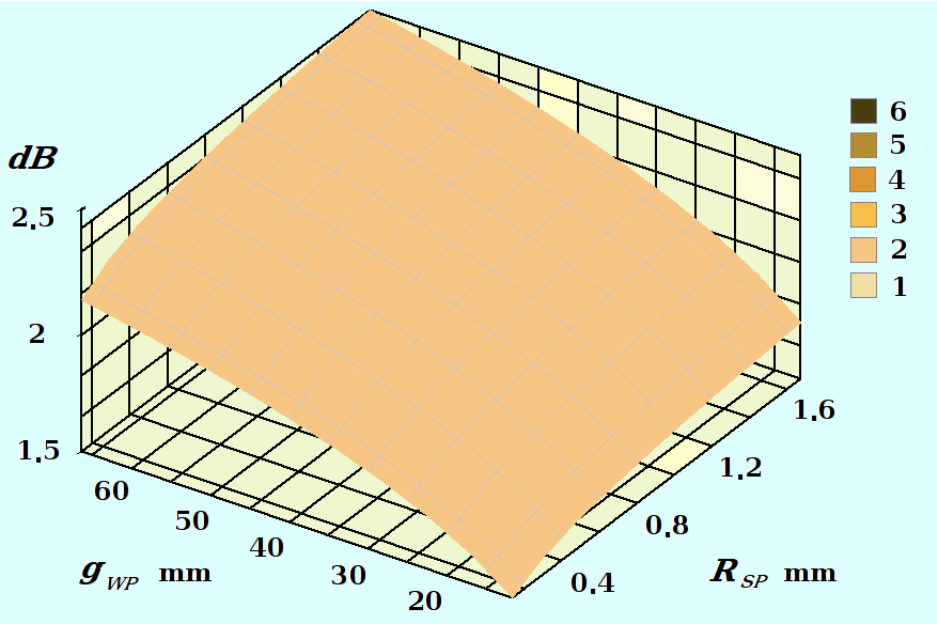

Fig. 5. Dependence between the degree of burning *dB* and the size of sanding grit R_{SP} and the thickness of sanding specimen g_{WP}, according to formula (3); sanding parameters: p_S = 0.0015 N/mm^2, b_{WP} = 82.4 mm, v_C = 24.6 m/s, a_R = 0.2 mm; t_S = 30 min, Σt_S = 30 min

It has to be mentioned that the sanding tool lost sanding capability after reaching the maximum degree of burning *dB* = 6, by filling up the void spaces between grits. In case of grit *no.* 160(12), debris collected inside the volume between grits, but was able to form exhaust aisles by itself during the next less intensive test. This occurrence was probably the main reason for a rather large variation of the observed sanding intensities $\Delta l_{WP}/\Delta t_S$.

For formula (4), involving the describing dependency $\Delta l_{WP}/\Delta t_S = f(Q_S, g_{WP}, b_{WP}, \rho_{SP}, R_{SP}, v_C, \Sigma t_S, a_R)$, the following estimators were evaluated: c_1 = 0.0803; c_2 = -1.50287;

c_3 = 1.43538; c_4 = -2.0223; c_5 = -2.65478; c_6 = 0.29524; c_7 = 2.09626; c_8 = -2.11·10^{-6}; c_9 = -0.00502; c_{10} = -0.00979; note: g_{WP} and b_{WP} are expressed in [cm].

The quality of approximation of the fit of formula (4) was shown in Fig. 6 and was also characterized by the quantifiers: S_K = 32.9; R = 0.98; R^2 = 0.95; S_D = 0.56 mm/min. The coefficients of relatively importance C_{RI} for estimators of formula (4) were as follows: C_{RI1} = 2260, C_{RI2} = 1793; C_{RI3} = 1098; C_{RI4} = 542313; C_{RI5} = 2.1·10^9; C_{RI6} = 832; C_{RI7} = 2257; C_{RI8} = 0.1; C_{RI9} = 0.1; $C_{RI\,10}$ =0.4.

Figure 7 shows that the sanding intensity $\Delta l_{WP}/\Delta t_S$ strongly depended upon the sanding load Q_S. Figure 6 also shows that the sanding intensity $\Delta l_{WP}/\Delta t_S$ significantly depended upon the sanding speed v_C for high values of the sanding load Q_S. An increase of the sanding speed v_C slightly increased the sanding intensity $\Delta l_{WP}/\Delta t_S$. This relation could not be observed for low values of the sanding load Q_S.

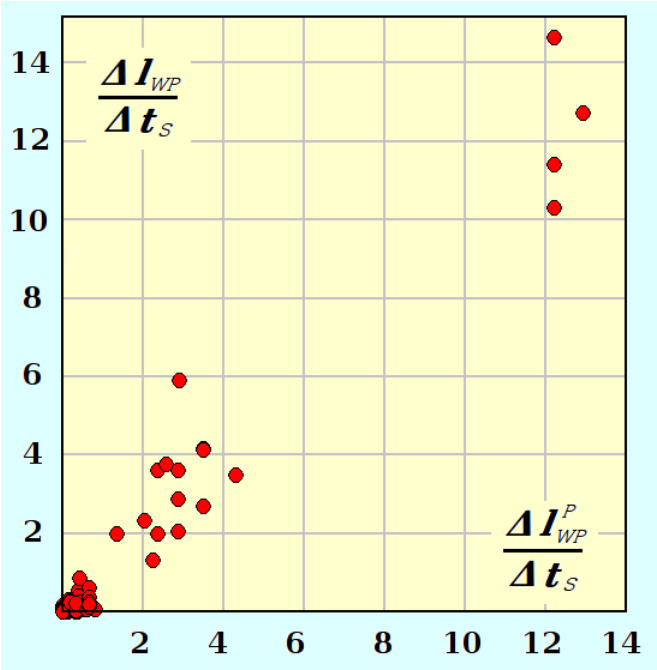

Fig. 6. The plot of the observed sanding intensity $\Delta l_{WP}/\Delta t_S$, against predicted $\Delta l_{WP}/\Delta t_S{}^P$, according to formula (4)

From Figs. 8 and 9 it can be seen that increasing the thickness g_{WP} as well as the width of sanding specimen b_{WP} hyperbolically decreased the sanding intensity $\Delta l_{WP}/\Delta t_S$. This was due to a decrease of sanding pressure p_S at the constant sanding load Q_S.

Figure 10 shows that the influence of the size of sanding grit R_{SP} on the sanding intensity $\Delta l_{WP}/\Delta t_S$ was rather small and visible for higher sanding pressure p_S. An increase of the size of sanding grit R_{SP} slightly increased the sanding intensity $\Delta l_{WP}/\Delta t_S$. Because it showed evidence of a combined influence of the size of sanding grit R_{SP} together with the rounding of the points of sanding grit ρ_{SP} defined by statistical formula (4) on the sanding intensity $\Delta l_{WP}/\Delta t_S$, the separate analysis of the ρ_{SP} on the $\Delta l_{WP}/\Delta t_S$ was omitted.

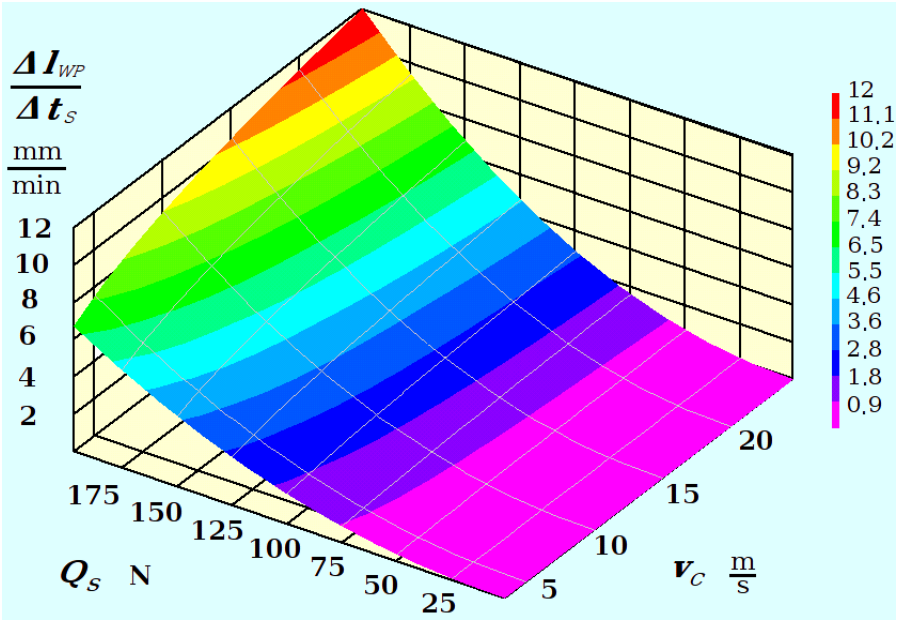

Fig. 7. Dependence between the sanding intensity $\Delta l_{WP}/\Delta t_S$ and the sanding speed v_C, and the sanding load Q_S, according to formula (4); sanding parameters: g_{WP} = 66.4 mm, b_{WP} = 10 mm, v_C = 3.45 m/s, R_{SP} = 1.67 mm, t_S = 10 min, Σt_S = 10 min, a_R = 0,13 mm

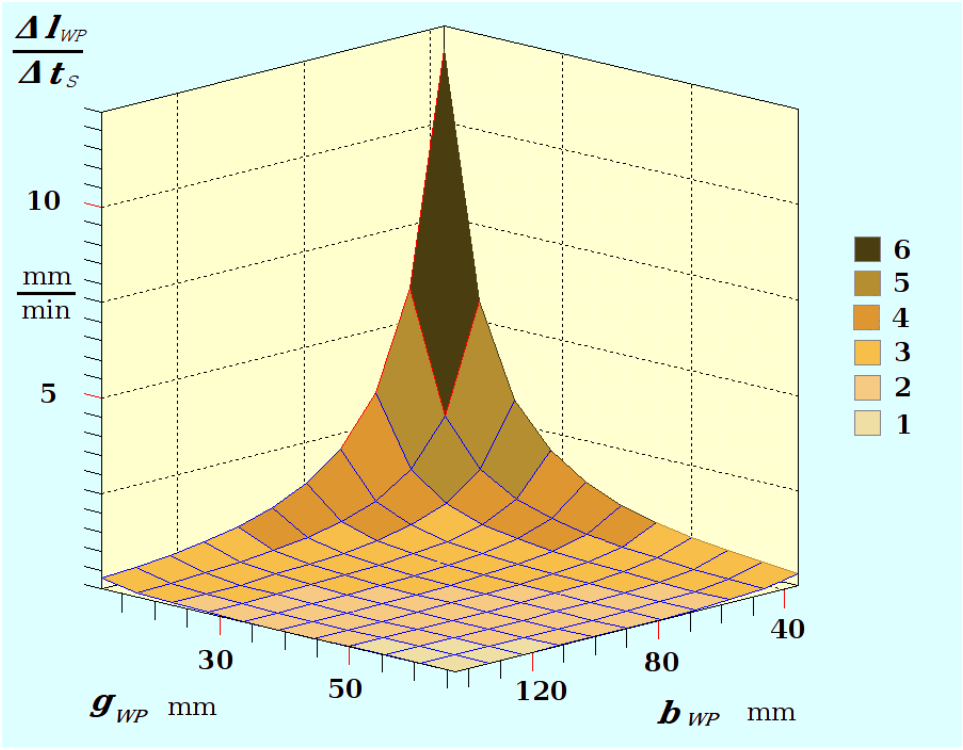

Fig. 8. Dependence between the sanding intensity $\Delta l_{WP}/\Delta t_S$ and the thickness g_{WP} and the width of sanding specimen b_{WP}, according to formula (4); sanding parameters: Q_S = 10 N; R_{SP} = 1.67 mm; t_S = 3 min; Σt_S = 3 min; a_R = 1.4 mm; v_C = 24.6 m/s

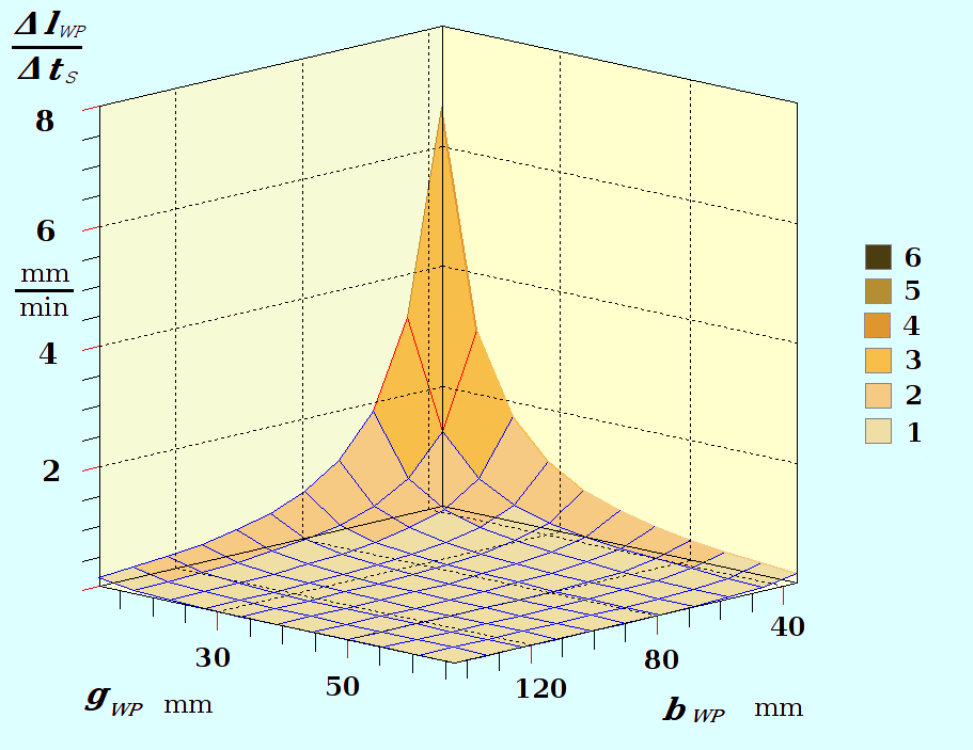

Fig. 9. Dependence between the sanding intensity $\Delta l_{WP}/\Delta t_S$ and the thickness g_{WP} and the width of sanding specimen b_{WP}, according to formula (4); sanding parameters: Q_S = 10 N; R_{SP} = 1.67 mm; t_S = 3 min; Σt_S = 3 min; a_R = 1.4 mm; v_C = 3.5 m/s

According to formula (4), an increase of the axial run out a_R of the sanding tool slightly decreased the sanding intensity $\Delta l_{WP}/\Delta t_S$ (on a low level of importance) (Fig. 10).

An increase of the size of sanding grit R_{SP} resulted in growth of the sanding intensity $\Delta l_{WP}/\Delta t_S$, with decreasing tendency (Fig.10). The significance of the influence of the R_{SP} on the sanding intensity $\Delta l_{WP}/\Delta t_S$, was lower than sanding load Q_S, and the thickness g_{WP} and the width b_{WP} of wooden specimen.

An increase of the total sanding operation time Σt_S also slightly decreased (on low level of importance) the sanding intensity $\Delta l_{WP}/\Delta t_S$. This was due to filling up of spaces between sanding particles by wood dust. This influence was much smaller than expected. A reason for this can be the large variation of sanding conditions applied in the tests. An example of that can be points numbers 39, 40, and 41 (Table 7, see Appendix). The sanding intensity $\Delta l_{WP}/\Delta t_S$ for point no. 41 was higher than for point no. 39, although the last point was observed for lower total sanding operation time Σt_S. This suggests that the spaces between sanding particles filled up earlier, but were for some reasons released after tests numbers 39 and 40, allowing an increase in sanding intensity $\Delta l_{WP}/\Delta t_S$ for test no. 41. Occurrences like that could be repeated randomly many times in the whole total sanding operating time Σt_S. Long, but dissimilar pauses between tests may also contribute to the phenomenon mentioned above.

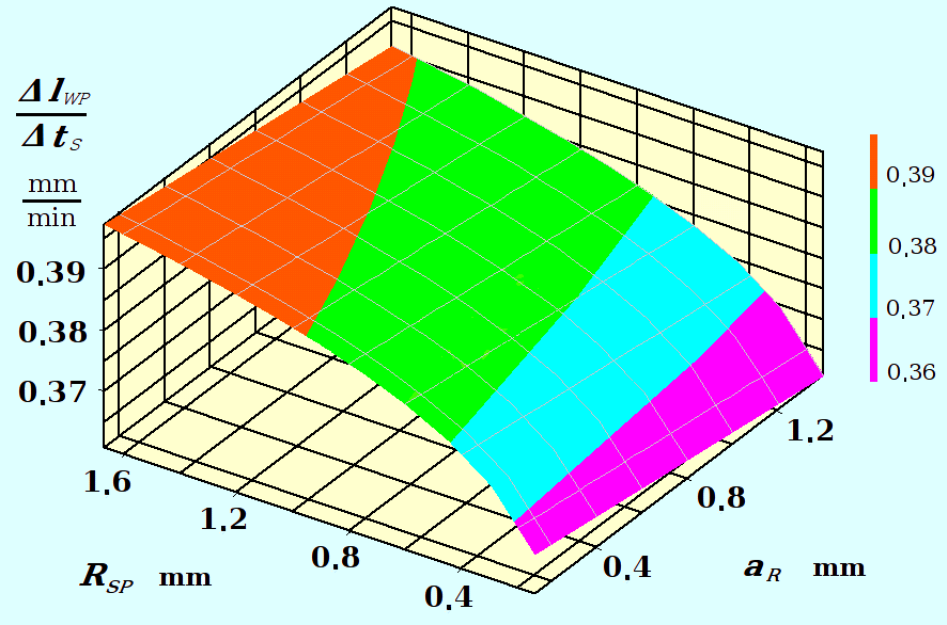

Fig. 10. Relation between the sanding intensity $\Delta l_{WP}/\Delta t_S$ and the size of sanding grit R_{SP} and axial run out of sanding tool a_R, according to formula (4); sanding parameters: Q_S = 2 N; v_C = 24.67 mm; t_S = 3 min; Σt_S = 3 min; a_R = 0.13 mm; v_C = 24.6 m/s

Although in the beginning of calculation, the time of a single sanding cycle t_S in formula (4) was showing evidence of an appreciable coefficient of relative importance C_{RI}, by the conclusion of the calculation the t_S term had been eliminated from the formula (4), by $C_{RI} << 0.1$. A reason for that can be the large variation of sanding conditions applied in the course of experiments.

It has to be mentioned that sanding of wood of *Fagus silvatica L.* perpendicularly to grains without burning marks can be made possible by limiting the sanding pressure p_S to suitably low values. During experiments, when using sanding grit no. 160(12) (R_{SP} = 1.67) and large sanding pressure p_S, on the lower edge of a wooden specimen, high, unacceptable stash was observed. Tables 4, 5, and 6 show collected sets of parameters for a fresh sanding tool. The acceptable sanding load Q_S, for the condition $dB < 1.5$ was evaluated from formulas (3) and (4). From Tables 4, 5, and 6, it can be seen that for sanding grit *nrs* 50(30) and 12(100), the acceptable (not causing burning marks) sanding load Q_S and sanding intensity $\Delta l_{WP}/\Delta t_S$, were larger in comparison to sanding grit *no.* 160(12). This was due to the fact that the grits *nrs* 50(30) and 12(100) were sharper than grit *no.* 160(12).

Table 4. Acceptable Sanding Load Q_S for Perpendicular Sanding of *Fagus silvatica L.* Wood Without Burning Marks ($dB < 1.5$), by: t_S = 1 min, Σt_S = 5 min, a_R = 0.2 mm

R_{SP} (mm)	A (mm^2)	b_{WP} (mm)	g_{WP} (mm)	v_C (m/s)	Q_S (N)	$\Delta l_{WP}/\Delta t_S$ (mm/min)
1.67	814	22	37	10	2.64	0.1328
1.67	2376	36	66	10	6.7	0.0694
1.67	5760	40	144	10	15.77	0.0383

Table 5. Acceptable Sanding Load Q_S for Perpendicular Sanding of *Fagus silvatica L.* Wood Without Burning Marks (dB < 1.5), by: t_S = 1 min, Σt_S = 5 min, a_R = 0.2 mm

R_{SP} (mm)	A (mm^2)	b_{WP} (mm)	g_{WP} (mm)	v_C (m/s)	Q_S (N)	$\Delta l_{WP}/\Delta t_S$ (mm/min)
0.57	814	22	37	10	2.89	0.1564
0.57	2376	36	66	10	7.31	0.0822
0.57	5760	40	144	10	17.18	0.0461

Table 6. Acceptable Sanding Load Q_S for Perpendicular Sanding of *Fagus silvatica L.* Wood Without Burning Marks (dB < 1.5), by: t_S = 1 min, Σt_S = 5 min, a_R = 0.2 mm

R_{SP} (mm)	A (mm^2)	b_{WP} (mm)	g_{WP} (mm)	v_C (m/s)	Q_S (N)	$\Delta l_{WP}/\Delta t_S$ (mm/min)
0.14	814	22	37	10	3.25	0.194
0.14	2376	36	66	10	8.19	0.10244
0.14	5760	40	144	10	19.26	0.0584

In order to avoid surface burning during sanding perpendicularly to the grains, it is recommended to apply low sanding load Q, that is equal to lower sanding pressure p_S, for sanding small dimensions (height g_{WP} and width b_{WP}) of the work piece. Rather than sanding out a necessary layer in one cycle, apply many shorter cycles separated by pauses. The sanded surface might be cooled down by putting it onto the machine table. Do not increase the sanding load for larger sanding speed v_C. Reduce the sanding pressure if one recognizes that the sanding grit that is going to be used is not sharp.

For future work, it would be recommended to use a sharper, large size sanding grit from a material other than electrocorunde, which was used in the present experiment for sanding of *Fagus silvatica L.* wood perpendicular to the grain.

CONCLUSIONS

1. Results from the analysis of the experiments performed showed that it is possible to sand perpendicular to grains wood of *Fagus silvatica L.* without burning marks (Tables 4, 5, and 6).
2. The level of burning of a sanded surface dB strongly depended upon sanding pressure p_S. An increase of the sanding pressure p_S increased the degree of burning dB.
3. The degree of burning dB depended upon sanding speed v_C. The increase of sanding speed v_C increased the degree of burning dB. This influence was small for low values of the sanding pressure p_S.
4. An increase of time of single sanding cycle t_S increased the degree of burning dB.
5. An increase of total sanding operation time Σt_S decreased the degree of burning dB.
6. The level of burning dB slightly increased with increasing the thickness of wood specimen g_{WP}. This influence can be seen for larger values of the sanding pressure p_S.
7. The level of burning dB slightly increased with increasing size of sanding grit R_{SP}. This influence could be seen for larger values of the sanding pressure p_S.

8. The sanding intensity $\Delta l_{WP}/\Delta t_S$ strongly depended upon the sanding load Q_S. An increase of the sanding load Q_S increased the sanding intensity $\Delta l_{WP}/\Delta t_S$.
9. The sanding intensity $\Delta l_{WP}/\Delta t_S$, at constant sanding pressure p_S, strongly depended upon the thickness of sanding specimen g_{WP}. An increase of the thickness of sanding specimen g_{WP} decreased hyperbolically the sanding intensity $\Delta l_{WP}/\Delta t_S$.
10. The sanding intensity $\Delta l_{WP}/\Delta t_S$, by constant sanding pressure p_S, strongly depended upon the width of sanding specimen b_{WP}. An increase of the width of sanding specimen b_{WP} decreased hyperbolically the sanding intensity $\Delta l_{WP}/\Delta t_S$.
11. The sanding intensity $\Delta l_{WP}/\Delta t_S$ depended upon sanding speed v_C. An increase of the sanding speed v_C increased the sanding intensity $\Delta l_{WP}/\Delta t_S$. This influence was observed for large values of the sanding speed v_C.
12. The sanding intensity $\Delta l_{WP}/\Delta t_S$ slightly depended upon the size of sanding grit R_{SP}. This influence could be seen for larger values of the sanding pressure p_S. An increase of the size of sanding grit R_{SP} increased the sanding intensity $\Delta l_{WP}/\Delta t_S$.

ACKNOWLEDGMENTS

The authors are grateful for the support of the Poznań Networking & Supercomputing Center (PCSS) calculation grant.

REFERENCES CITED

Orlicz, T. (1982). "Obróbka drewna narzędziami tnącymi," (Machining of wood with use of cutting tools), *Study book SGGW-AR*, Warsaw (in Polish).

Pahllitzsch, G., and Dziobek, K. (1961). "Über das Wesen der Abstumpfung von Schleifenbänder beim Bandschleifen von Holz," *Holz als Roh und Werkstoff* V19, 136 - 149.

Porankiewicz, B. (1988). "Mathematical model of edge dullness for prediction of wear of wood cutting tool," *9 Wood Machining Seminar*, University of California, Forest Products Laboratory, Richmond, USA, 169 - 170.

Schmutzler, W. (1961). "Zur Technologie des Breitband Kontaktschleifens," *Holz als Roh und Werkstoff* V19(4), 153 - 159.

Article submitted: March 20, 2008; Peer-review completed: April 24, 2008; Revised version received: April 25, 2008; Article accepted: April 26, 2008; Published: May 3, 2008.

APPENDIX

Table 7. The Complete Experimental Matrix

No	t_S	a_R	ρ_{SP}	R_{SP}	g_{WP}	B_{WP}	v_C	Q_S	Σt_S	$\Delta l_{WP}/\Delta t_S$	dB
	(min)	(mm)	(mm)	(mm)	(mm)	(mm)	(m/s)	(N)	(min)	(mm/min)	-
1	30.0	0.40	0.23	1.67	35.6	66.6	3.5	5.2	30.0	0.0001	1
2	30.0	0.13	0.23	1.67	35.6	66.6	3.5	3.2	60.0	0.0003	1
3	30.0	0.13	0.23	1.67	35.6	66.6	3.5	3.2	90.0	0.00001	1
4	30.0	0.18	0.23	1.67	35.6	66.6	3.5	5.2	120.0	0.001	1
5	30.0	0.18	0.23	1.67	35.6	66.6	3.5	5.2	150.0	0.00001	1
6	30.0	0.18	0.23	1.67	35.6	66.6	3.5	5.2	180.0	0.00001	1
7	30.0	0.18	0.23	1.67	35.6	66.6	3.5	8.1	210.0	0.00001	1
8	30.0	0.18	0.23	1.67	35.6	66.6	3.5	8.1	240.0	0.00001	1
9	30.0	0.18	0.23	1.67	35.6	66.6	3.5	8.1	270.0	0.00001	1
10	30.0	0.41	0.23	1.67	35.6	66.6	10.4	3.2	30.0	0.0017	1
11	30.0	0.41	0.23	1.67	35.6	66.6	10.4	3.2	60.0	0.00001	1
12	30.0	0.41	0.23	1.67	35.6	66.6	10.4	3.2	90.0	0.00001	1
13	30.0	0.4	0.23	1.67	35.6	66.6	10.4	5.2	120.0	0.0001	1
14	30.0	0.4	0.23	1.67	35.6	66.6	10.4	5.2	150.0	0.0017	2
15	30.0	0.4	0.23	1.67	35.6	66.6	10.4	5.2	180.0	0.0017	1
16	0.083	0.25	0.23	1.67	35.6	66.4	10.4	32.6	184.563	1.32	2
17	30.0	0.4	0.23	1.67	35.6	66.6	10.4	8.1	210.0	0.0003	3
18	30.0	0.4	0.23	1.67	35.6	66.6	10.4	8.1	240.0	0.00001	3
19	30.0	0.4	0.23	1.67	35.6	66.6	10.4	8.1	270.0	0.0013	3
20	0.5	0.42	0.08	0.57	40.6	144.1	13.5	98.8	14.5	2.0	5
21	0.067	0.42	0.08	0.57	40.6	144.1	13.5	98.8	14.576	3.6	5
22	3.0	0.42	0.08	0.57	40.6	144.1	13.5	49.4	17.576	0.07	4
23	12.0	0.5	0.23	1.67	26.0	67.0	16.8	13.0	33.0	0.1259	5
24	30.0	0.96	0.23	1.67	35.6	66.6	16.8	3.2	75.0	0.0017	1
25	20.0	0.8	0.23	1.67	35.6	66.6	16.8	5.2	95.0	0.0017	2
26	20.0	0.8	0.23	1.67	35.6	66.6	16.8	8.1	115.0	0.0017	3
27	5.0	0.5	0.23	1.67	35.6	66.6	16.8	13.0	120.0	0.02	3
28	5.0	0.5	0.23	1.67	35.6	66.6	16.8	13.0	125.0	0.01	3
29	5.0	0.5	0.23	1.67	35.6	66.6	16.8	13.0	130.0	0.02	3
30	10.0	0.5	0.23	1.67	35.6	66.6	16.8	13.0	140.0	0.005	4
31	10.0	0.5	0.23	1.67	35.6	66.6	16.8	13.0	150.0	0.015	4
32	10.0	0.5	0.23	1.67	35.6	66.6	16.8	13.0	160.0	0.02	4

33	20.0	0.5	0.23	1.67	35.6	66.6	16.8	13.0	180.0	0.016	4
34	0.083	0.4	0.23	1.67	35.6	66.4	16.8	32.6	184.48	3.75	3
35	20.0	0.5	0.23	1.67	35.6	66.6	16.8	3.2	210.0	0.00001	1
36	30.0	0.96	0.23	1.67	35.6	66.6	16.8	3.2	240.0	0.0033	1
37	30.0	0.8	0.23	1.67	35.6	66.6	16.8	5.2	270.0	0.0117	2
38	30.0	0.8	0.23	1.67	35.6	66.6	16.8	5.2	300.0	0.01	2
39	10.0	0.5	0.23	1.67	11.8	66.5	16.8	13.0	310.0	1.695	5
40	10.0	0.5	0.23	1.67	11.8	66.5	16.8	13.0	320.0	4.16	5
41	10.0	0.5	0.23	1.67	11.8	66.5	16.8	13.0	330.0	4.135	5
42	3.0	0.42	0.08	0.57	23.8	66.5	17.1	13.0	38.0	0.0733	2
43	3.0	0.42	0.08	0.57	23.8	66.5	17.1	13.0	41.0	0.0567	2
44	3.0	0.42	0.08	0.57	23.8	66.5	17.1	13.0	44.0	0.05	2
45	3.0	0.36	0.02	0.14	35.1	66.1	24.6	3.2	3.0	0.1633	1
46	3.0	0.36	0.02	0.14	35.1	66.1	24.6	3.2	6.0	0.15	1
47	3.0	0.36	0.02	0.14	35.1	66.1	24.6	3.2	9.0	0.1043	1
48	3.0	0.36	0.02	0.14	35.1	66.1	24.6	3.2	12.0	0.0667	1
49	3.0	0.36	0.02	0.14	35.1	66.1	24.6	3.2	15.0	0.051	1
50	3.0	0.36	0.02	0.14	35.1	66.1	24.6	3.2	18.0	0.0233	1
51	1.0	0.38	0.02	0.14	35.1	66.1	24.6	8.1	19.0	0.216	1
52	1.0	0.38	0.02	0.14	35.1	66.1	24.6	8.1	20.0	0.294	1
53	1.0	0.38	0.02	0.14	35.1	66.1	24.6	8.1	21.0	0.1633	1
54	1.0	0.40	0.02	0.14	35.1	66.1	24.6	13.0	22.0	0.49	1
55	1.0	0.4	0.02	0.14	35.1	66.1	24.6	13.0	23.0	0.55	1
56	1.0	0.4	0.02	0.14	35.1	66.1	24.6	13.0	24.0	0.394	1
57	3.0	0.38	0.02	0.14	35.1	66.1	24.6	5.2	42.0	0.0943	1
58	3.0	0.38	0.02	0.14	35.1	66.1	24.6	5.2	45.0	0.0577	1
59	3.0	0.38	0.02	0.14	35.1	66.1	24.6	5.2	48.0	0.1022	1
60	5.0	0.29	0.08	0.57	35.1	66.1	24.6	3.2	5.0	0.0192	1
61	5.0	0.29	0.08	0.57	35.1	66.1	24.6	3.2	10.0	0.006	1
62	5.0	0.29	0.08	0.57	35.1	66.1	24.6	3.2	15.0	0.022	1
63	5.0	0.34	0.08	0.57	35.1	66.1	24.6	5.2	20.0	0.028	1
64	5.0	0.34	0.08	0.57	35.1	66.1	24.6	5.2	25.0	0.018	1
65	5.0	0.34	0.08	0.57	35.1	66.1	24.6	5.2	30.0	0.014	1
66	5.0	0.34	0.08	0.57	35.1	66.1	24.6	5.2	35.0	0.016	1
67	5.0	0.42	0.08	0.57	35.1	66.1	24.6	8.1	40.0	0.116	1
68	5.0	0.42	0.08	0.57	35.1	66.1	24.6	8.1	45.0	0.058	1
69	5.0	0.42	0.08	0.57	35.1	66.1	24.6	8.1	50.0	0.058	1

70	3.0	0.42	0.08	0.57	35.1	66.1	24.6	13.0	53.0	0.2333	2
71	4.8	0.42	0.08	0.57	35.1	66.1	24.6	13.0	57.8	0.2396	1
72	3.0	0.42	0.08	0.57	35.1	66.1	24.6	13.0	60.8	0.1533	3
73	3.0	0.42	0.08	0.57	35.1	66.1	24.6	13.0	63.8	0.24	3
74	10.0	1.4	0.23	1.67	11.8	66.5	24.6	1.2	10.0	0.00001	1
75	10.0	1.4	0.23	1.67	11.8	66.5	24.6	1.2	20.0	0.01	1
76	10.0	1.4	0.23	1.67	11.8	66.5	24.6	1.2	30.0	0.00001	1
77	10.0	1.1	0.23	1.67	11.8	66.5	24.6	3.2	40.0	0.275	2
78	10.0	1.1	0.23	1.67	11.8	66.5	24.6	3.2	50.0	0.24	2
79	10.0	1.1	0.23	1.67	11.8	66.5	24.6	3.2	60.0	0.25	2
80	10.0	0.75	0.23	1.67	11.8	66.5	24.6	5.2	70.0	0.155	3
81	10.0	0.75	0.23	1.67	11.8	66.5	24.6	5.2	80.0	0.085	3
82	10.0	0.75	0.23	1.67	11.8	66.5	24.6	5.2	90.0	0.12	3
83	10.0	0.70	0.23	1.67	23.8	66.5	24.6	8.1	100.0	0.0126	4
84	10.0	0.7	0.23	1.67	23.8	66.5	24.6	8.1	110.0	0.0251	4
85	10.0	0.7	0.23	1.67	23.8	66.5	24.6	8.1	120.0	0.0189	4
86	0.122	0.6	0.23	1.67	11.7	66.6	24.6	22.8	183.872	12.74	6
87	0.142	0.6	0.23	1.67	35.6	66.4	24.6	22.8	184.013	1.98	2
88	0.133	0.6	0.23	1.67	71.3	66.7	24.6	22.8	184.147	0.225	2
89	0.128	0.6	0.23	1.67	35.6	66.4	24.6	13.0	184.275	0.8571	2
90	0.15	0.6	0.23	1.67	66.4	35.6	24.6	13.0	184.713	0.07	2
91	0.112	0.6	0.23	1.67	35.6	66.4	24.6	32.6	184.386	5.91	4
92	0.09	0.6	0.23	1.67	66.4	35.6	24.6	22.8	184.803	2.33	3
93	0.097	0.6	0.23	1.67	66.4	35.6	24.6	32.6	184.9	3.48	4
94	0.083	0.6	0.23	1.67	40.8	144.1	24.6	49.4	184.983	0.6	3
95	0.083	0.6	0.23	1.67	40.8	144.1	24.6	49.4	185.067	0.36	3
96	0.083	0.6	0.23	1.67	40.8	144.1	24.6	49.4	185.15	0.24	3
97	0.333	0.6	0.23	1.67	40.8	144.1	24.6	49.4	185.483	0.18	4
98	0.333	0.6	0.23	1.67	40.8	144.1	24.6	49.4	185.817	0.12	4
99	0.333	0.6	0.23	1.67	40.8	144.1	24.6	49.4	186.15	0.18	4
100	0.083	0.6	0.23	1.67	40.8	144.1	24.6	98.8	186.233	3.6	5
101	0.083	0.6	0.23	1.67	40.8	144.1	24.6	98.8	186.317	2.04	5
102	0.083	0.6	0.23	1.67	40.8	144.1	24.6	98.8	186.40	2.88	5
103	0.083	0.6	0.23	1.67	40.8	144.1	24.6	196.9	186.483	10.32	6
104	0.083	0.6	0.23	1.67	40.8	144.1	24.6	196.9	186.576	11.4	6
105	0.083	0.6	0.23	1.67	40.8	144.1	24.6	196.9	186.65	14.64	6